J Appl Electrochem (2013) 43:1185–1195
DOI 10.1007/s10800-013-0596-4

RESEARCH ARTICLE

The effect of thiourea, L(−) cysteine and glycine additives on the mechanisms and kinetics of copper electrodeposition

Bogale Tadesse · Michael Horne · Jonas Addai-Mensah

Received: 6 May 2013 / Accepted: 21 July 2013 / Published online: 6 September 2013

Abstract The influence of thiourea, L(−) cysteine and glycine on the mechanisms and kinetics of copper electrodeposition from aqueous solution at pH 1.00 ± 0.05 and 25 °C was investigated using several complementary techniques. Rotating disc electrode current density measurements and the kinetic parameters calculated from Koutecký–Levich analysis indicated that at 5×10^{-3} M thiourea and L(−) cysteine addition the electro-reduction of Cu(II) was significantly inhibited. By contrast, upon similar addition of glycine, the reduction current density increased and the equilibrium potential moved towards more positive values. Microscopic imaging studies of the resulting Cu films showed that thiourea and L(−) cysteine led to fine-grained deposits, whilst glycine addition resulted in a coarser deposit. It is suggested the additives substantially altered the electron and mass transfer processes during electrodeposition. Both thiourea and L(−) cysteine appear to act by specific chemical interactions that lead to CuS co-crystallization. On the other hand, glycine is believed to act by mediating the Cu(II) to Cu(I) reduction process.

Keywords Mechanisms and kinetics · Electrodeposition · Copper · Thiourea · L(−) Cysteine · Glycine

B. Tadesse · J. Addai-Mensah (✉)
Ian Wark Research Institute, ARC Special Research Centre for Particles and Interfaces, University of South Australia, Mawson Lakes Campus, Mawson Lakes, Adelaide, SA 5095, Australia
e-mail: jonas.addai-mensah@unisa.edu.au

M. Horne
CSIRO Process Science and Engineering, Box 312, Clayton South, Melbourne, VIC 3168, Australia

1 Introduction

Electrodeposition from aqueous solutions is an inexpensive and versatile technique used to produce high-quality metal and coated metal products [1]. Deposits with various physicochemical properties may be achieved with high selectivity so long as the primary variables such as current density (applied potential), bath composition and temperature are carefully tuned [2, 3]. As a result, electrodeposition is widely used in corrosion protection, electroplating, electrorefining and electrowinning of high-purity metals [4]. Recently, electroplating has gained great practical significance in the electronic industry for the fabrication of interconnects in printed circuit boards, integrated chips and magnetic layers [5, 6].

Controlling the adhesion, crystallite size and porosity, and surface roughness of the electrodeposited film is, however, not straightforward and the details of processes developed for industrial applications are frequently well-guarded secrets. High current densities and/or pulsed current are sometimes used to obtain deposits with high electrical conductivities, high strengths and improved surface qualities [7]. However, it is also well known that the addition of small concentrations of some organic additives to electrodeposition baths leads to striking changes in the nature of metallic deposits recovered at the cathode. For instance, the damascene process for electrodepositing copper into the fine and tortuous channels which comprise the vias or interconnects on a printed circuit board use a number of additives which increase the 'throwing power' of the deposition bath [8]. In the electrorefining industry thiourea (TU) is commonly used as grain refiner [8–11] because it increases the nucleation rate and promotes electrodeposition in recesses [8]. It has also been reported that TU may be involved in various reactions in the solution phase with Cu^{2+} resulting in Cu^{+} intermediate species [8]. Yet other

studies suggest that TU decomposes into H_2S which then reacts with Cu(II) to form insoluble species such as CuS [10, 12] which interferes with normal crystal growth by blocking active sites and preventing surface integration at the cathodic surface. However, TU also inhibits the kinetics of copper electrodeposition [10] and because it is also toxic, alternatives for electrorefining applications are in demand. Two which show some promise are the amino acids, L(−) cysteine (CYS) and glycine (GLY). Literature concerning the impact of (CYS) and (GLY) on copper electrodeposition is limited and little kinetic data exists; it has been suggested from cathode polarization measurements that CYS may behave in a similar way as TU and may have inhibition/grain refining effect on copper electrodeposition [12]. CYS can be electrochemically reduced to generate sulphide ions which lead to the formation of CuS at the cathode surface, significantly reducing the rate of crystal growth [12]. On the other hand, GLY is known to be a levelling agent in copper electroplating even though its mechanism of action does not involve a significant change in kinetics of copper electrodeposition [12]. Gelatine [13], polyethylene glycol [14, 15] and benzotriazole [16] are also added for beneficial effects such as brightening and levelling of deposit. It has been reported that these substances are capable of influencing mass or charge transfer at electrode/electrolyte interfaces by forming adsorbed layers, complex species and precipitates [12, 17].

In order to understand how additives impact on the electrowinning or electrorefining of metals, it is crucial to identify the main processes involved. The processes occurring include diffusion of electroactive ions to the electrode/electrolyte interface, charge transfer, formation of critical nuclei and the incorporation of adatoms into a crystal lattice. Organic additives may act by interfering with one or more of these processes, and may affect the overall electrodeposition phenomena and hence the nature of the metallic deposit.

Although it has been established that additives have the aforementioned benefits, there is a limited understanding on their mechanism of action and little kinetic information exists on the overall electrodeposition process [4, 5, 8, 18, 19]. The main objective of this study is to investigate the influence of TU, GLY and CYS on the mechanisms and kinetics of electrodeposition of copper onto gold electrode. The impact of these additives on charge transfer, reaction rate and diffusion of Cu(II) species as well as surface morphology and the structure of Cu deposits will be probed.

2 Experimental section

A standard three-electrode system comprising a 5-mm-diameter gold disc working electrode (0.196 cm^2), a 10-cm-long platinum wire (0.5 mm diameter) counter electrode and a Ag|AgCl|KCl(satd.) system reference electrode was used. These and the electrochemical glass cell used were supplied by Pine Research Instrumentation (USA). For the atomic force microscopy (AFM) imaging and X-ray photoelectron spectroscopy (XPS) analysis, silicon wafer plates (1.0 cm^2) coated with 50-nm-thick gold were used as substrate for electrodeposition.

Acidic Cu(II) sulphate electrolyte solutions used were prepared with analytical grade copper sulphate (Chem supply) and sulphuric acid (Lab-scan) and adjusted to the desired pH using 2 M sodium hydroxide (MERCK Pty Limited). TU (M & B), GLY (Unilab) and CYS (Sigma) were used as additives by dissolving known amounts into 10^{-2} M $CuSO_4$ solution. Due to some common functional groups containing –S and –N atoms (Fig. 1) CYS, GLY and TU may be expected to behave in similar ways.

Voltammetric measurements were made using an Autolab Potentiostat/Galvanostat PGSTAT30 (Eco Chemie, The Netherlands) interfaced with a PC using GPES software. In each test, 60 cm^3 of the electrolyte solution was added into a 125 cm^3 electrochemical glass cell. Each test was replicated at least 6 times. The working electrodes were mechanically polished to a mirror finish before and after electrodeposition using 1.0 and 0.05 μm alumina suspensions (Buehler) and rinsed with high-purity Milli-Q water (pH 5.6, surface tension 72 mN m^{-1} and resistivity of 18.2 MΩ cm) produced by a Barnstead NANOpure purification system. Applied potentials ranging from −0.20 to −0.50 V versus Ag|AgCl|KCl(satd.) were used for constant potential deposition based on voltammetric tests recorded between +0.3 and −0.6 V at scan rate of 20 mV s^{-1}. A rotating disc electrode (0.196 cm^2) was used to study mass transfer processes at rotation speeds of 0, 200, 400, 600, 800, 1,000 and 1,200 rpm. Experiments involving the electrodeposition of copper in acidic solution were conducted at pH 1.0 and 25 °C. In the presence of the additives, the pH of the solution did not change significantly with variations measured in the range of ±0.05.

Multimode 8 AFM (Bruker, Germany) with a 'J' scanner was used to probe the surface topography of copper deposits. The samples were prepared by electrodeposition of Cu on a gold-plated silicon wafer at a potential of

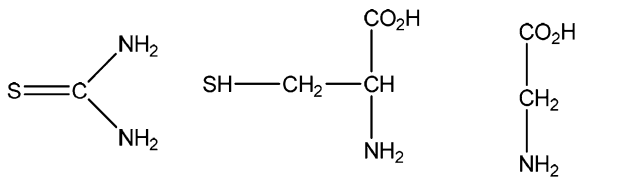

Thiourea (TU) mol. mass 76.14 | Cysteine (CYS) mol. mass 121.18 | Glycine (GLY) mol. mass 75.08

Fig. 1 Structural formulae of the three additives with their respective molar masses (amu)

−0.40 V, removed immediately from the electrolyte solution, rinsed with Milli-Q water and allowed to dry at room temperature. Then, *ex-situ* AFM images were obtained in ScanAsyst™ mode where imaging parameters were automatically adjusted by decoupling cantilever response from resonance dynamics which allowed uniformly optimized feedback loop for all points of the heterogeneous surface through the control of direct interaction force. To investigate the nature and composition of metallic Cu deposited in the presence of the additives, XPS analysis was performed. The samples were prepared by electrodeposition of Cu on Au at a constant potential of −0.40 V [vs. Ag|AgCl|KCl(sat'd)] applied for 5 min in the absence and presence of the additives. After electrodeposition, the samples were rinsed with Milli-Q water and dried at room temperature before the XPS analysis. The XPS analysis was done using a Kratos Axis Ultra with delay-line detector and the spectra were interpreted using the Casa-XSP software package.

3 Results and discussion

3.1 Electrocrystallization under quiescent conditions

In order to investigate the influence of CSY, GLY and TU on the mechanisms and kinetics of copper electrodeposition on gold, linear scan voltammetry (LSV) experiments were carried out in 10^{-2} M $CuSO_4$ solutions containing no additives or 5×10^{-3} M of CSY, GLY and TU. The resulting voltammograms are shown in Fig. 2. The applied potential scan commenced at +0.3 V and was reversed at −0.6 V. In the absence of the additives, a typical electrodeposition wave was recorded, with a peak current density of −1.6 mA cm^{-2} at −0.26 V which then diminished as $t^{1/2}$ signalling a diffusion-controlled process (Fig. 2, curve a). The reduction of Cu^{2+} to Cu^0 has been reported to proceed in two steps given by R_1 and R_2 [20].

$$Cu^{2+} + e^- \rightarrow Cu^+ \text{ (slow)} \quad \text{(R1)}$$

$$Cu^+ + e^- \rightarrow Cu^0 \text{ (fast)} \quad \text{(R2)}$$

In the presence of GLY, the maximum reduction current (Fig. 2, curve b, point III) occurs at a slightly less negative potential than without additives and the voltammogram also shows a preceding shoulder at about −0.08 V (Fig. 2, curve b, point II). The shoulder is most probably due to the formation of Cu^+–GLY complex following reaction R_1. This complex does form [21, 22] and its binding energy has been calculated to be 69 kcal mol^{-1} [23]. On the other hand, in the presence of CYS the reduction current density was significantly smaller at 1.1 mA cm^{-2} and a broader curve was observed, which suggests that the kinetics of Cu electrodeposition were sluggish (Fig. 2, curve c). The addition of TU shifted the deposition potential to more negative values as may be seen from Fig. 2, curve d, suggesting this additive inhibits deposition.

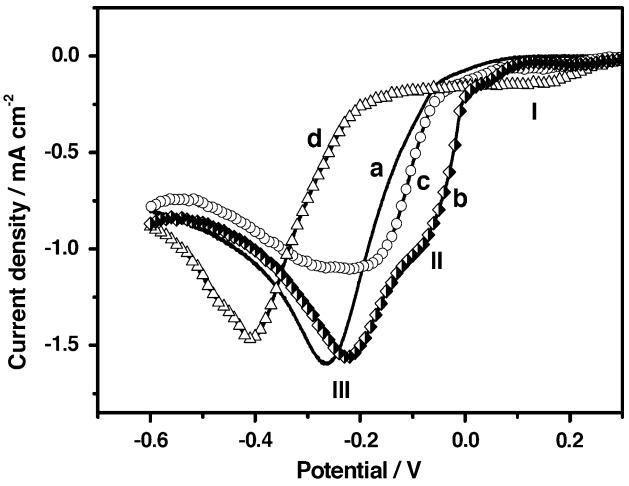

Fig. 2 Linear scan voltammograms recorded for Cu electrodeposition on Au disc electrode from 10^{-2} M $CuSO_4$ (pH 1.0) at scan rate of 20 mV s^{-1} *a* no additives and in the presence of 5×10^{-3} M, *b* GLY, *c* CYS and *d* TU

3.2 Electrocrystallization under convective (hydrodynamic) conditions

Further investigation of the kinetic changes in the reduction of copper in the presence of the organic additives was performed using a rotating disc electrode (RDE). To compare the processes taking place at the RDE with that at a stationary electrode, linear sweep voltammograms were obtained at 1,000 rpm (Fig. 3). The j–E curves show similar kinetic behaviour with that of the stationary case given in Fig. 2. Compared with the voltammogram obtained for the additive-free solution (Fig. 3, a), the limiting currents did not attain a true steady-state in the presence of additives even at very high overpotentials, which might suggest the existence of other processes such as adsorption and precipitation in addition to mass transfer control.

3.2.1 Diffusion coefficient of Cu(II) species

3.2.1.1 Levich method The application of the Levich equation (Eq. 1) to determine diffusion coefficient during electrodeposition is well discussed in the literature [9, 24–28].

$$i_{l,c} = 0.62nFAD^{2/3}\omega^{1/2}\nu^{-1/6}C \quad (1)$$

where $i_{l,c}$ (A) is the limiting current (in a laminar flow regime), n is the number of electrons transferred, F (C mol^{-1}) is Faraday's constant, A (cm^2) is the electrode disc area, D (cm^2 s^{-1}) is the diffusion coefficient,

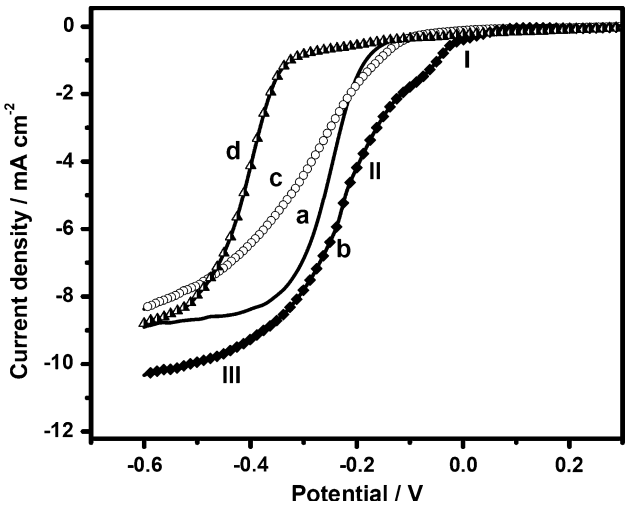

Fig. 3 Linear scan voltammograms recorded for Cu electrodeposition on Au rotating disc electrode at 1,000 rpm from *a* 10^{-2} M $CuSO_4$ solution and in the presence of 5×10^{-3} M of *b* GLY, *c* CSY and *d* TU. Scan rate is 20 mV s^{-1}

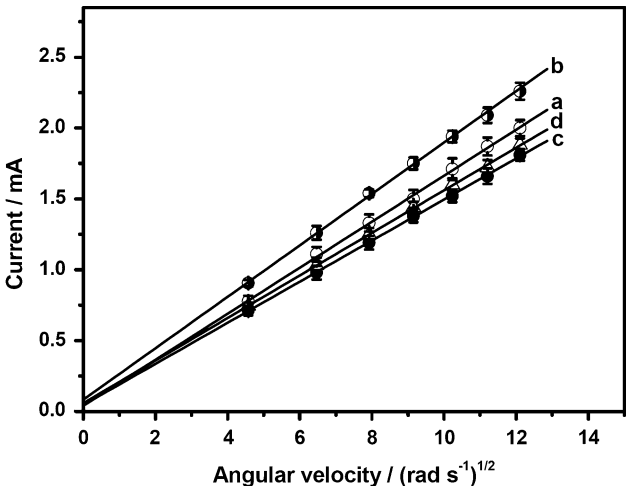

Fig. 4 Levich plots for Cu electrodeposition from 10^{-2} M $CuSO_4$ in H_2SO_4 (pH 1.0) *a* in the absence of additive and in the presence of 5×10^{-3} M, *b* GLY, *c* CYS and *d* TU

ω (rad s^{-1}) is the electrode rotation rate, v (cm^2 s^{-1}) is viscosity of electrolyte solution and C (mol cm^{-3}) is the bulk concentration of electroactive species [e.g. Cu(II)]. This equation applies to mass transport-limited reactions which have fast electron transfer kinetics [25, 29, 30], although other work has shown that it may be applied outside this strict limitation [9, 28].

Nevertheless, Quickenden and Jiang [26] reported that the use of Levich equation to determine diffusion coefficient of Cu(II) ions from aqueous sulphate solution is appropriate only over a narrow range of potential as the evolution of H_2 at high overpotentials makes a significant contribution to the current. To deal with this problem in the current work, cathodic currents were measured at −0.50 V for all rotation speeds (200, 400, 600, 800, 1,000, 1,200 and 1,400 rpm), where the overpotential is in high enough to ensure that Cu(II) reduction is under diffusion control but low enough that H_2 evolution occurs at a very low rate (see Fig. 1). The resulting plots of $i_{l,c}$ versus $\omega^{1/2}$ in the presence and absence of additives are shown in Fig. 4. From the slopes of these plots, diffusion coefficients were estimated and are given in Table 1. These results show small variation and are in good agreement with similar systems reported in the literature [9, 27]. For instance, differences of 1.7 % for 5×10^{-2} M $CuSO_4$ [30], 10.3 % for 10^{-3} M $CuSO_4$ in 0.5 M H_2SO_4 and 4.9 % for a solution containing 5×10^{-6} to 1×10^{-3} M TU in 1×10^{-3} M $CuSO_4$ were observed [9].

3.2.1.2 Koutecky–Levich method According to Quickenden and Xu [27], the values of diffusion coefficients determined by the Levich method can be significantly lower than their real values due to the presence of charge transfer processes not considered by the Eq. 1. Thus, it is of interest to estimate the values of D using other methods and compare them with those obtained using Levich method. The Koutecky–Levich method may be employed alternatively for the determination of D values of Cu(II) [27] where the mixed control form given by Eq. 2 is used to account for both activation (charge transfer) and mass transport polarizations. In the present work, the values of the current (i) were taken for various rotation rates (400–1,200 rpm) at various applied potentials ranging from −0.20 to −0.50 V, i.e. from region II in Fig. 3, where the electrodeposition process is assumed to be under both charge and mass transfer control. However, it should be noted that for the case of TU, applied potentials of −0.40, −0.45 and −0.50 V were chosen as indicated in Fig. 5 to account for the mixed control region as the cathodic potential was shifted significantly to more negative values.

$$\frac{1}{i} = \frac{1}{i_K} + \frac{1}{i_{l,c}} = \frac{1}{i_K} + \frac{1}{0.62nFAD^{2/3}\omega^{1/2}v^{-1/6}C} \quad (2)$$

where i_k (A) represents the current due to only kinetically limited processes and is given by [24]:

Table 1 Diffusion coefficients of Cu^{2+} in 10^{-2} M $CuSO_4$ at pH 1.0 in the absence and presence of 5×10^{-6} M GLY, CYS and TU estimated by the Levich equation

Additive type	$D \times 10^6$ (cm^2 s^{-1})	R^2
–	6.10 ± 0.37	0.999
CYS	5.16 ± 0.48	0.998
GLY	7.10 ± 0.18	0.999
TU	5.36 ± 0.17	0.999

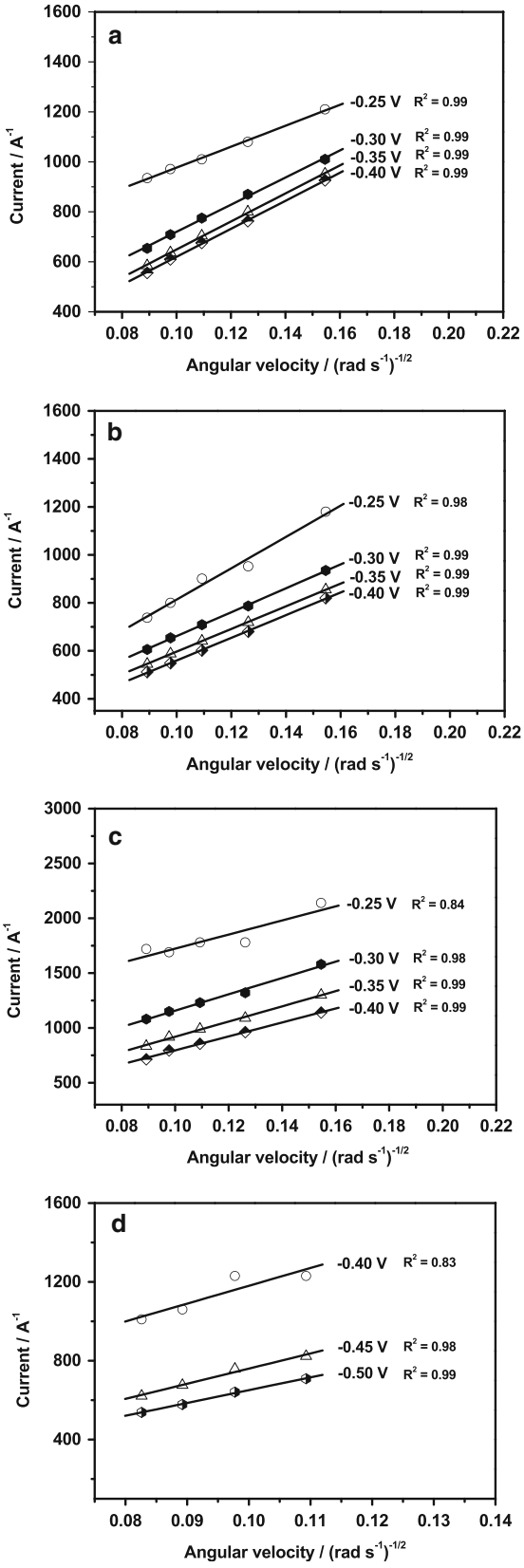

Fig. 5 Koutecky–Levich plots for Cu electrodeposition on Au rotating disc electrode from **a** 10^{-2} M $CuSO_4$ solution and in the presence of 5 × 10^{-3} M of **b** GLY, **c** CYS and **d** TU

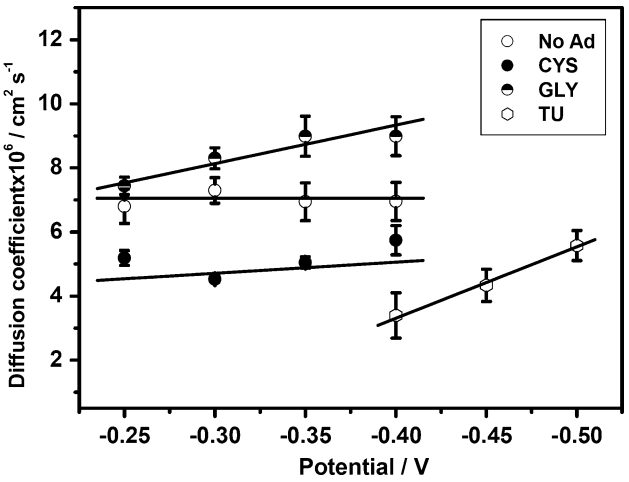

Fig. 6 Diffusion coefficients values of Cu(II) calculated using Koutecky–Levich method (mixed control region) at various applied potentials in the absence and presence of additives

$$i_{\mathrm{K}} = FAk^0C\exp\left(\frac{-\alpha_{\mathrm{c}}F\eta}{RT}\right) \tag{3}$$

where k^0 (cm s^{-1}) is the standard rate constant, α_c is the cathodic transfer coefficient, η (V) is the overpotential, R (J K^{-1} mol^{-1}) is the universal gas constant and T (K) is the absolute temperature. A plot of i^{-1} versus $\omega^{-1/2}$ should be linear as given in Fig. 5 and values of D can be obtained from the slopes at each applied potential. While small differences in D were observed with applied potential, larger differences resulted when different additives were used (Fig. 6). The diffusion coefficient is smallest in the presence of TU, slightly larger when CYS is added and greatest in the presence of GLY. The values of D calculated by this method are about 10 % higher than those estimated using the Levich equation for no additive, CYS and GLY but lower for TU.

3.2.2 *Estimation of kinetic parameters: k^0 and α_c*

The reduction of Cu(II) to Cu(I) is the slowest of the two steps in the overall reduction reaction. The standard heterogeneous rate constant k^0 and the transfer coefficient α_c for this process were estimated from the mixed potential response of a rotating disc electrode using Koutecky–Levich method in the presence of additives. From the y-axis intercepts in Fig. 5, values of the kinetically limited current i_k were calculated (shown in Fig. 7) and k^0 and α_c were then estimated from the plots of ln i_k versus η as given in Table 2.

It can be seen from that the standard heterogeneous rate constant (k^0) varies over two orders of magnitude, from a value of 0.25 × 10^{-5} cm s^{-1} in the presence of TU (in which deposition is inhibited), to a value of 118 × 10^{-5} cm s^{-1} in the presence of GLY (in which deposition

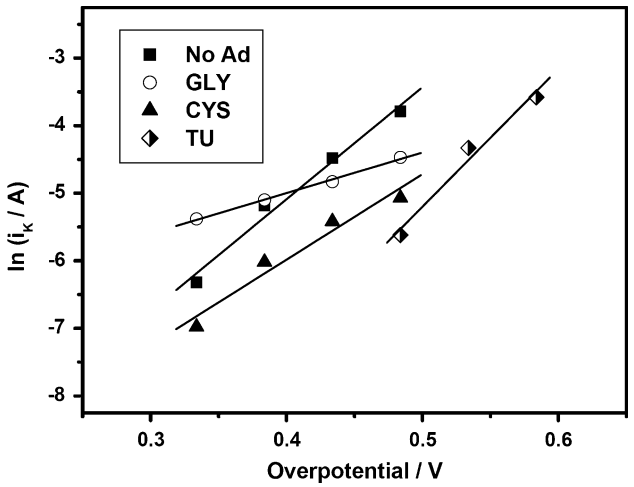

Fig. 7 Plots of the kinetics limited current versus overpotential (Tafel-type representation) in the absence and in the presence of 5×10^{-3} M additives

Table 2 Kinetic parameters calculated (with standard deviation) using Koutecky–Levich method for reduction of copper (R_1) in the absence and presence of GLY, CYS and TU

Additive type	Transfer coefficient (α_c)	Standard rate constant $k^0 \times 10^5$ (cm s^{-1})	R
–	0.51 ± 0.01	3.93 ± 0.44	0.998
CYS	0.40 ± 0.01	6.49 ± 0.18	0.999
GLY	0.25 ± 0.02	118 ± 13	0.997
TU	0.48 ± 0.02	0.24 ± 0.01	0.998

is strongly facilitated). However, k^0 also increased in the presence of CYS even though the overall reduction process was inhibited when this additive was used. This most likely results from the formation of a stable complex between CYS and Cu(I) [31] which increases the rate of Cu(II) reduction, but inhibits the rate of Cu(I) reduction. Pecci et al. [31] have reported that in the presence of CYS, Cu(I) forms cuprous bis-cysteine complex of the form [CYS–Cu(I)–CYS] according to reaction 4 given in Sect. 3.3.3. At lower overpotentials and higher CYS concentrations (10^{-3} and 10^{-2} M), it has also been shown that a stable Cu(I)–CYS intermediate exists in an acidic sulphate solution [32]. A higher value of k^0 ($10.9 \pm 0.1 \times 10^{-5}$ cm s^{-1}) was obtained for pure 0.5 M $CuSO_4$ [19] which is reasonable, as heterogeneous electrodeposition rate is expected to be higher for concentrated systems [9].

In the absence of additives, the charge transfer coefficient for Cu(II) was found to be 0.51 ± 0.01 (Table 2), in close agreement with values of 0.50 for 1×10^{-3} to 5×10^{-3} M Cu(II) and 0.49 ± 0.01 for 0.5 M Cu(II) reported elsewhere [9, 19]. In the presence of 5×10^{-3} M TU, the charge transfer coefficient was estimated as 0.48 ± 0.02. Values of 0.35 in the presence of 5×10^{-6} to 5×10^{-4} M TU and 0.26 in the presence of 1×10^{-3} M TU were reported [9]. Smaller values were calculated for CYS and GLY. The substantial decrease in cathodic charge transfer coefficient in the presence of additives may suggest a more complex electrodeposition process.

3.3 Morphological analysis

The presence of additives in the electrodeposition bath significantly influences the grain size and roughness of copper deposits. Figure 8a–e shows AFM images obtained before and after copper electrodeposition using a fixed potential of −0.40 V for 5 min. From Fig. 8a, it is possible to observe that the pristine gold substrate has a relatively smooth surface (RMS < 2 nm). Upon electrodeposition of copper in the absence of additives, a large number of crystals emerged (Fig. 8b), and a 2D growth was observed covering the whole surface. This behaviour most likely arises because of the strong deposit–substrate interaction and little crystallographic mismatch between Au and Cu [33]. The addition of CYS reduces the grain size and, therefore, produces a smoother Cu deposit, as shown in Fig. 8c. The most striking impact was observed in the presence of TU, where crystal aggregates were formed (Fig. 8d). By contrast, the addition of GLY caused a slight increase in the deposit grain size and roughness compared with the additive-free deposit (Fig. 8e). These observations are in good agreement with the electrochemical results where GLY facilitates copper electrodeposition, whereas CYS and TU inhibit the same reaction.

3.3.1 Deposit surface chemical composition analysis

Copper surfaces deposited in the presence of CYS and TU were found by XPS to contain CuS-based species, as indicated by the S 2p doublet spectra peaks at binding energy ~162.8 and 164.0 eV (Fig. 9c, d). The prominent doublet observed in the presence of CYS may be attributed to similar chemical environment of sulphur bonded to Cu such as Cu–S [19]. Likewise, the small but noticeable S 2p spectrum indicated in the presence of TU corresponds to CuS species formed at the surface, the concentration of which is lower than that CYS. In the absence of these 2 additives, no such S 2p peaks were observed (Fig. 9a, b). In all samples, a small peak was observed at 168.3 eV due to the incorporation of sulphate species from the electrolyte solution (not shown in Fig. 9 for clarity).

Nitrogen lone-pairs on amine moieties within an additive are commonly implicated in chemisorption onto Cu surfaces [34]. Such adsorbates are stable [35] and may even be incorporated in the Cu metal deposit. In the XPS spectra of Cu films produced in the presence GLY, CYS and TU, N 1 s peaks were observed at 398.5 eV, as shown in Fig. 10.

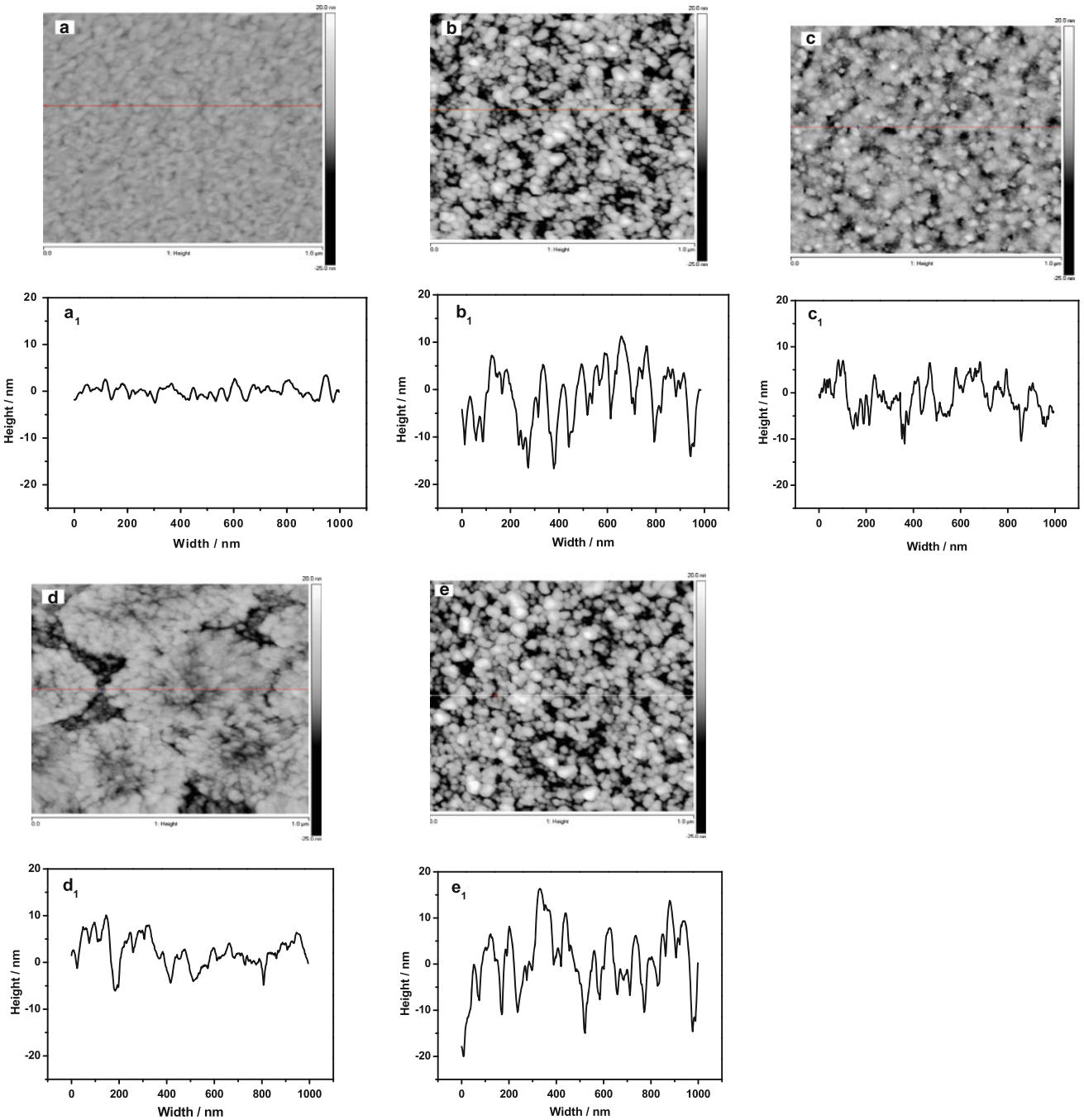

Fig. 8 AFM images of **a** pristine Au electrode and Cu films electrodeposited at a potential of −0.40 V from an aqueous 10^{-2} M $CuSO_4$ solution (pH 1.0) and in the presence, **b** no additive, **c** CYS, **d** TU and **e** GLY

This peak, attributed to N–Cu interactions, is noticeably more intense for Cu films obtained in the presence of CYS and TU than that of GLY. This observation suggests stronger, specific interactions (e.g. chemisorption) of CYS and TU with Cu species or their direct incorporation into the Cu crystal lattice [34, 35]. The other peak component that appears at 400.1 eV is ascribed to N atoms in the additive molecules (e.g. $–NH_2$) which seems to proliferate Cu deposit surface in the presence of CYS and to a lesser extent, GLY.

3.3.2 Mechanism of action of TU

The mechanism of action of TU on copper electrodeposition from acidic solutions has been intensively studied

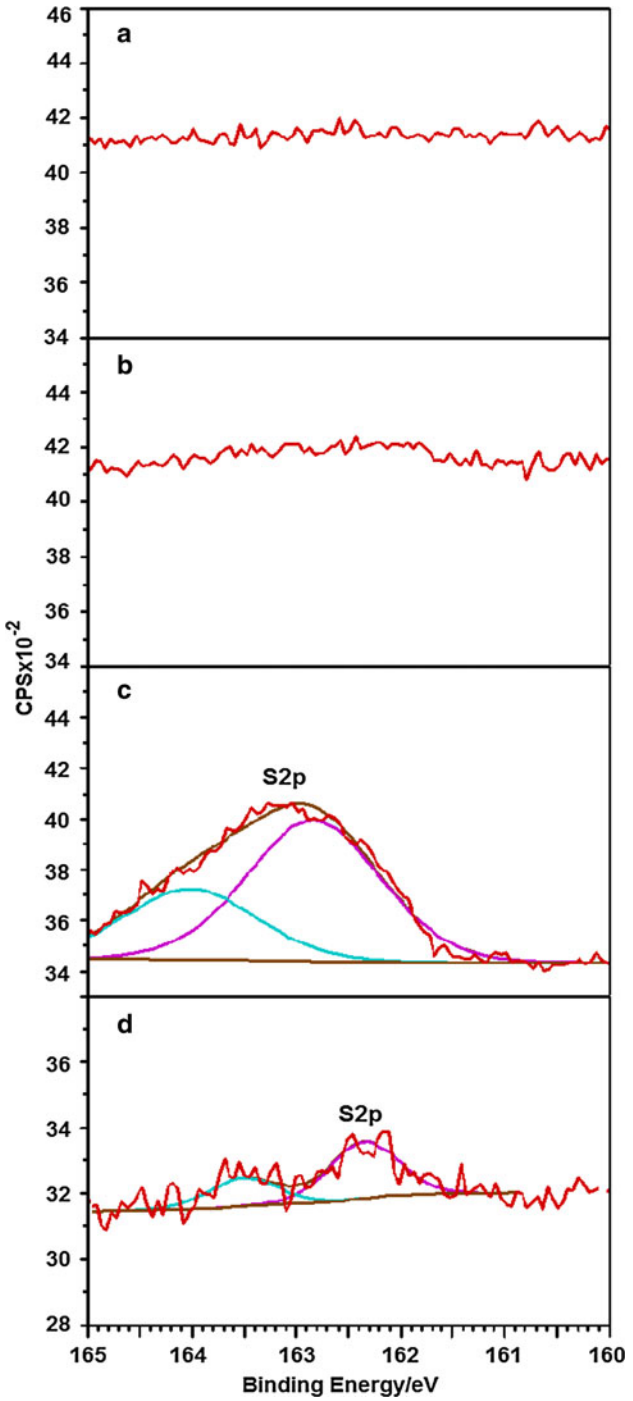

Fig. 9 XPS spectra for S recorded on Cu deposited onto Au electrodes at a potential of −0.40 V for 5 min from **a** 10^{-2} M $CuSO_4$ and in the presence 5×10^{-3} M of **b** GLY, **c** CYS and **d** TU

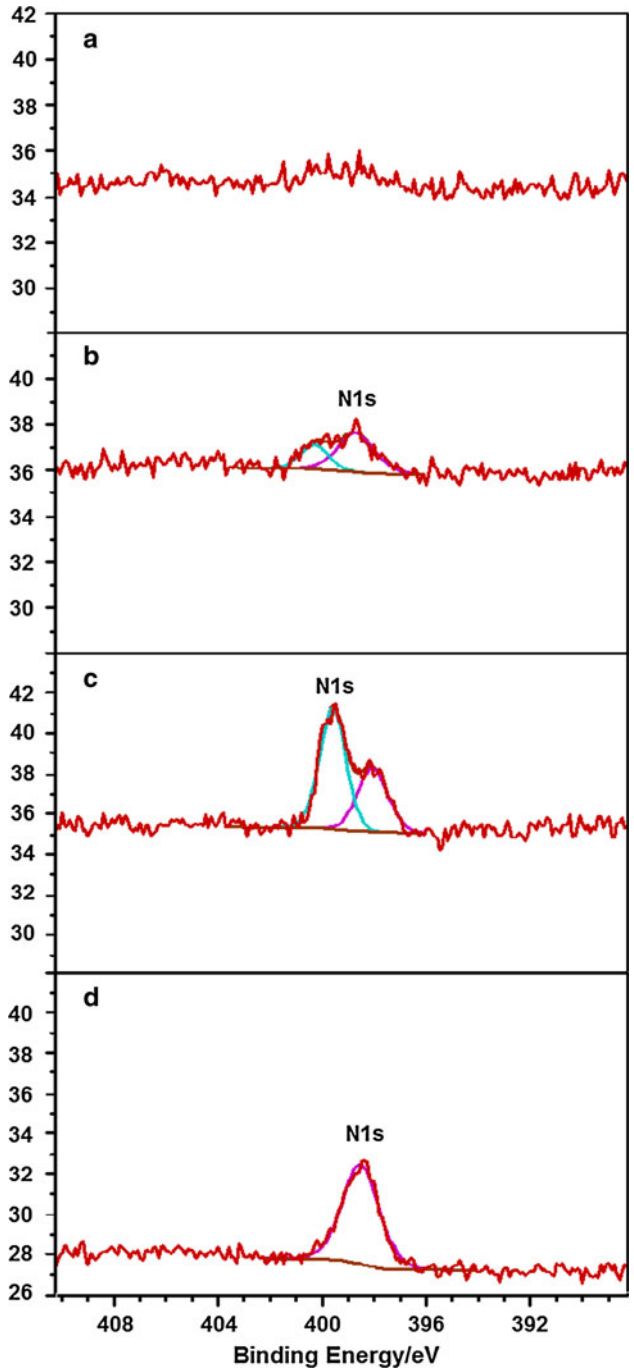

Fig. 10 XPS spectra for N recorded on Cu deposited onto Au electrodes at a potential of −0.40 V for 5 min from **a** 10^{-2} M $CuSO_4$ and in the presence 5×10^{-3} M of **b** GLY, **c** CYS and **d** TU

[9, 10, 12, 17], but the exact mechanism remains unclear. One possibility is that TU decomposes into H_2S which then reacts with Cu^{2+} to form insoluble CuS [10, 12]. Other studies found no evidence of CuS incorporation into the deposited Cu film and concluded that TU does not participate in the interfacial electrochemical reactions [17].

This work shows that there is a significant decrease in the deposition current density in the presence of TU compared with an additive-free solution (Figs. 2, 3) and AFM studies revealed substantial grain size reduction in the Cu deposits (Fig. 8d). Moreover, the appearance of voids between the crystal aggregates supports a previous

hypothesis that the precipitation/adsorption of insoluble species onto areas of high current density slows the rate of nucleation and growth at these sites [12]. The formation of CuS at the electrode surface is confirmed in this study by XPS analyses. Thus, TU is involved in Cu electrodeposition either by adsorption onto the electrode surface or by complexing Cu ions in solution. In either case, incorporation of TU into the copper film inhibits nucleation and growth substantially. The reaction of TU with copper ions, the generation of CuS and subsequently blocking the electrode surface has been reported elsewhere [10].

3.3.3 Mechanism of action of CYS

The electrochemical and morphological studies suggest that like TU, CYS acts as an inhibitor, for copper electrodeposition and produces fine-grained deposits. Several mechanisms may be responsible for the action of CYS on this process. At sufficiently high CYS concentrations, Cu^{2+} undergoes reductive complexation with CYS [31] to form:

$$6HSCH_2CHNH_2COOH + 2Cu^{2+} \rightarrow 2Cu^{+}\ (SCH_2CHNH_2COOH)_2 + HOOCNH_2CHCH_2S - SCH_2CHNH_2COOH + 6H^{+} + 4e^{-} \quad (4)$$

Thus, the plating solution in the presence of CYS may contain various intermediate complexes which may also incorporate solvent molecules. Hence, the overall rate of electrodeposition will be controlled by the reduction kinetics of these intermediate species [36]. The formation of stable intermediate complexes can often slow rate of electrodeposition. The substantially lower current density observed during the electrodeposition of copper in the presence of CYS is in accordance with this mechanism.

Moreover, CYS can undergo oxidation to cystine according to the following reaction [37]:

$$HSCH_2CHNH_2COOH + HSCH_2CHNH_2COOH \rightarrow HOOCNH_2CHCH_2S - SCH_2CHNH_2COOH + 2H^{+} \quad (5)$$

This process is greatly augmented by transition metals such as copper [38]. Both CYS and cystine can be electrochemically reduced to generate sulphide ions which, in turn, could potentially form a strong bond with Cu^{2+}. The presence of such insoluble product at the cathode surface interferes with normal crystal growth and leads to grain refining [12]. The analysis of the composition of Cu deposit in our study indicated the co-precipitation of CuS species in the presence of CYS. A more uniform, compact and fine-grained deposit was obtained by CYS addition (Fig. 8c) which may be due to a preference of the intermediate products to adsorb at, or incorporate into the active lattice sites on the electrode surface. The strong adsorption of thiol side chain containing amino acids such as CYS on metallic surfaces has been investigated using in situ spectro-electrochemical methods [39].

3.3.4 Mechanism of action of GLY

The addition of GLY in this study was found to facilitate copper electrodeposition. In order to understand the mechanism, the data collected in this study, together with knowledge of the equilibrium forms of GLY in acidic solutions must be carefully considered. First, this study shows that the addition of 5×10^{-3} M GLY alters the diffusion coefficient for Cu^{2+} by a slight amount but increases k^0 for the reduction of Cu(II) to Cu(I) by 25 times. This, together with the observation that the charge transfer coefficient is also strongly affected indicates that GLY can accelerate the kinetics of the slow step in the overall process: the initial reduction of Cu(II) to Cu(I). However, it is likely that adsorption of GLY onto the copper surface also plays a role. In aqueous solutions, GLY may be present in different forms depending on the pH of the solution [40]:

$$H_3^{+}NCH_2COOH \leftrightarrow H_2NCH_2COOH + H^{+} \quad pKa = 2.47 \quad (6)$$

$$H_2NCH_2COOH \leftrightarrow H_2NCH_2COO^{-} + H^{+} \quad pKa = 9.66 \quad (7)$$

At the pH of 1.0 (this study), the equilibrium form given in Eq. 6 is expected to occur. GLY is a relatively small molecule with functional groups containing electron-rich donor atoms—nitrogen and oxygen—which are sterically available for interaction with the copper surface. Brown et al. [41] have shown using surface-enhanced Raman spectroscopy that amide nitrogen atoms in gelatine effectively adsorb at a copper electrode immersed in sulphuric acid solution. Moreover, Chen et al. [42] report that GLY adsorbs on Au surfaces through both O atoms of the COO group in a bridge-bonded configuration. The adsorption of GLY on Au surfaces has also been observed in acidic media [43]. Unlike TU and CYS, GLY does not contain S atom and the formation of an insoluble product at the electrode/electrolyte interface is not expected to occur. Instead, an enhanced Cu(II) to Cu(I) reduction process and Cu crystal growth were favoured and hence, grain size increase as observed.

4 Conclusions

The effect of TU, CYS and GLY on the mechanisms and kinetics of electrodeposition of copper from acidic copper sulphate solution has been investigated. The voltammetric

measurements showed that the rate of copper electrodeposition increased in the presence of GLY but decreased with the addition of CYS and TU. The addition of GLY also resulted in a substantial decrease in charge transfer coefficient, suggesting that in this case, the electrodeposition process is complex. The rate constants estimated in the presence of the additives vary significantly due to various Cu(II) to Cu(I) reduction mechanisms involved. The estimated Cu(II) diffusion coefficient are smaller in the presence of TU and CYS and higher in the presence of GLY in comparison with the value for the additive-free solution. Morphological studies revealed that the addition of GLY resulted in a slight Cu deposit coarsening whilst CYS and TU led to remarkably fine-grained deposits. Specific interactions between the additives and either the electroactive Cu(I/II) or the electrode surface account for the observed additive-mediated Cu electrocrystallization processes and differing behaviour.

Acknowledgments The financial support from the Commonwealth Scientific and Industrial Research Organisation (CSIRO), the Ian Wark Research Institute and the University of South Australia are gratefully acknowledged. Discussions with L/Prof. J. Ralston and A/Prof. D. Fornasiero are greatly appreciated. The invaluable assistance provided by Dr. B. Follink from CSIRO is also gratefully acknowledged.

References

1. Schwarzacher W, Lashmore DS (1996) Giant magnetoresistance in electrodeposited films. IEEE T Magn 32:3133–3153
2. Huang L, Lee E-S, Kim K-B (2005) Electrodeposition of monodisperse copper nanoparticles on highly oriented pyrolytic graphite electrode with modulation potential method. Colloids Surf A 262:125–131
3. Natter H, Hempelmann R (2003) Tailor-made nanomaterials designed by electrochemical methods. Electrochim Acta 49: 51–61
4. Moats MS, Hiskey JB, Collins DW (2000) The effect of copper, acid, and temperature on the diffusion coefficient of cupric ions in simulated electrorefining electrolytes. Hydrometallurgy 56:255–268
5. Quiroga AMB, Vázquez CI, Lacconi GI (2010) Copper electrodeposition onto hydrogenated Si(111) surfaces: influence of thiourea. J Electroanal Chem 639:95–101
6. Stangl M, Acker J, Oswald S et al (2007) Incorporation of sulfur, chlorine, and carbon into electroplated Cu thin films. Microelectron Eng 84:54–59
7. Natter H, Hempelmann R (1996) Nanocrystalline copper by pulsed electrodeposition: the effects of organic additives, bath temperature, and pH. J Phys Chem 100:19525–19532
8. Vereecken PM, Binstead RA, Deligianni H, Andricacos PC (2005) The chemistry of additives in damascene copper plating. IBM J Res Dev 49:3–18
9. Farndon EE, Walsh FC, Campbell SA (1995) Effect of thiourea, benzotriazole and 4,5-dithiaoctane-1,8-disulphonic acid on the kinetics of copper deposition from dilute acid sulphate solutions. J Appl Electrochem 25:574–583
10. Kang MS, Kim S-K, Kim K, Kim JJ (2008) The influence of thiourea on copper electrodeposition: adsorbate identification and effect on electrochemical nucleation. Thin Solid Films 516: 3761–3766
11. Quinet M, Lallemand F, Ricq F et al (2009) Influence of organic additives on the initial stages of copper electrodeposition on polycrystalline platinum. Electrochim Acta 54:1529–1536
12. Turner DR, Johnson GR (1962) The effect of some addition agents on the kinetics of copper electrodeposition from a sulfate solution. J Electrochem Soc 109:798–804
13. Alvarez AE, Salinas DR (2004) Nucleation and growth of Zn on HOPG in the presence of gelatine as additive. J Electroanal Chem 566:393–400
14. Ballesteros JC, Diaz-Arista P, Meas Y, Ortega R, Trejo G (2007) Zinc electrodeposition in the presence of polyethylene glycol 20000. Electrochim Acta 52:3686–3696
15. Bonou L, Eyraud M, Denoyel R, Massiani Y (2002) Influence of additives on Cu electrodeposition mechanisms in acid solution: direct current study supported by non-electrochemical measurements. Electrochim Acta 47:4139–4148
16. Leung TYB, Kang M, Corry BF, Gewirth AA (2000) Benzotriazole as an additive for copper electrodeposition influence of triazole ring substitution. J Electrochem Soc 147:3326–3337
17. Alodan M, Smyrl W (1998) Effect of thiourea on copper dissolution and deposition. Electrochim Acta 44:299–309
18. Pletcher D, Whyte I, Walsh FC, Millington JP (1991) Reticulated vitreous carbon cathodes for metal ion removal from process streams part II: removal of Cu(II) from acid sulphate media. J Appl Electrochem 21:667–671
19. Varvara S, Muresan L, Popescu IC, Maurin G (2003) Kinetics of copper electrodeposition in the presence of triethyl-benzyl ammonium chloride. J Appl Electrochem 33:685–692
20. Mattsson E, Bockris JOM (1959) Galvanostatic studies of the kinetics of deposition and dissolution in the copper + copper sulphate system. Trans Faraday Soc 55:1586–1601
21. Hoyau S, Ohanessian G (1997) Absolute affinities of α-amino acids for Cu^{+} in the gas phase. A theoretical study. J Am Chem Soc 119:2016–2024
22. Bertrán J, Rodríguez-Santiago L, Sodupe M (1999) The different nature of bonding in Cu^{+}–glycine and Cu^{2+}–glycine. J Phys Chem B 103:2310–2317
23. Shoeib T, Rodriquez CF, Siu KWM, Hopkinson AC (2001) A comparison of copper(I) and silver(I) complexes of glycine, diglycine and triglycine. Phys Chem Chem Phys 3:853–861
24. Bard BJ, Faulkner LR (1980) Electrochemical methods: fundamentals and applications. Wiley, New York
25. Pletcher D, Greff R, Peat R, Peter LM (2001) Instrumental methods in electrochemistry. Ellis Horwood, Chichester
26. Quickenden TI, Jiang X (1984) The diffusion coefficient of copper sulphate in aqueous solution. Electrochim Acta 29:693–700
27. Quickenden TI, Xu Q (1996) Toward a reliable value for the diffusion coefficient of cupric ion in aqueous solution. J Electrochem Soc 143:1248–1253
28. Tindall GW, Bruckenstein S (1968) Determination of heterogeneous equilibrium constants by chemical stripping at a ring-disk electrode. Evaluation of the equilibrium constant for the reaction Cu + Cu(II) to 2Cu(I) in 0.2 M sulfuric acid. Anal Chem 40:1402–1404
29. Hinatsu JT, Foulkes FR (1989) Diffusion coefficients for Cu(II) in aqueous cupric sulfate–sulfuric acid solutions. J Electrochem Soc 136:125–132
30. MacHardy SJ, Janssen LJJ (2004) The diffusion coefficient of Cu(II) ions in sulfuric acid-aqueous and methanesulfonic acid–methanol solutions. J Appl Electrochem 34:169–174
31. Pecci L, Montefoschi G, Musci G, Cavallini D (1997) Novel findings on the copper catalysed oxidation of cysteine. Amino Acids 13:355–367
32. Matos JB, Pereira LP, Agostinho SML (2004) Effect of cysteine on the anodic dissolution of copper in sulfuric acid medium. J Electroanal Chem 570:91–94

33. Milchev A (2002) Electrocrystallization: fundamentals of nucleation and growth. Kluwer Academic Publishers, Boston
34. Rodriguez JA, Campbell CT (1988) A quantum-chemical study of the adsorption of water, formaldehyde and ammonia on copper surfaces and water ZnO(0001). Surf Sci 197:567–593
35. Rodriguez JA, Campbell RA, Corneille JS, Goodman DW (1991) The effects of CO, H, NH_3, CH_3OH, H_2O and C_2H_4 on the electronic properties of ultrathin Cu films supported over Ru(0001): an XPS study. Chem Phys Lett 180:139–144
36. Franklin TC (1987) Some mechanisms of action of additives in electrodeposition processes. Surf Coat Technol 30:415–428
37. Ralph TR, Hitchman ML, Millington JP, Walsh FC (1994) The electrochemistry of L-cystine and L-cysteine: Part 1: thermodynamic and kinetic studies. J Electroanal Chem 375:1–15
38. Majidi M, Asadpour-Zeynali K, Hafezi B (2010) Sensing L-cysteine in urine using a pencil graphite electrode modified with a copper hexacyanoferrate nanostructure. Microchim Acta 169: 83–288
39. Brolo AG, Germain P, Hager G (2002) Investigation of the adsorption of L-cysteine on a polycrystalline silver electrode by surface-enhanced Raman scattering (SERS) and surface-enhanced second harmonic generation (SESHG). J Phys Chem B 106:5982–5987
40. Messer BM, Cappa CD, Smith JD et al (2005) pH dependence of the electronic structure of glycine. J Phys Chem B 109: 5375–5382
41. Brown GM, Hope GA, Schweinsberg DP, Fredericks PM (1995) SERS study of the interaction of thiourea with a copper electrode in sulphuric acid solution. J Electroanal Chem 380:161–166
42. Chen L, Uchida T, Chang H, Osawa M (2013) Adsorption and oxidation of glycine on Au electrode: an in situ surface-enhanced infrared study. Electrochem Commun 34:56–59
43. Sandoval AP, Orts JM, Rodes A, Feliu JM (2011) Adsorption of glycine on Au(hkl) and gold thin film electrodes: an in situ spectroelectrochemical study. J Phys Chem C 115:16439–16450